

Symmetry Adapted Analysis of the Hoberman Switch-Pitch Ball

Yao CHEN
PhD candidate
Southeast University
Nanjing, CHN
chenyao_seu@hotmail.com

Simon D. GUEST
Reader
University of Cambridge
UK
sdg@eng.cam.ac.uk

Patrick W. FOWLER
Professor
University of Sheffield
UK
P.W.Fowler@sheffield.ac.uk

Jian FENG
Professor
Southeast University
Nanjing, CHN
fengjian@seu.edu.cn

Abstract

The Hoberman Switch-Pitch ball is used as the inspiration for a symmetry analysis of a novel type of deployable structure. The underlying structure of the Switch-Pitch is essentially cubic, consisting of eight nodes that are connected via revolute joints to twelve linking bars, each of which is connected to two nodes. A simple mobility count suggests that the structure is over-constrained, but a symmetry mobility analysis shows that the structure is in fact mobile, and retains tetrahedral symmetry as it folds.

Keywords: *symmetry; self-stress; mechanism; revolute joint; compatibility matrix.*

1. Introduction

Deployable structures or mechanisms having a single degree of freedom that allows them to change their shape are an important component of many civil engineering and aerospace systems. However, finding novel example of such structures is difficult. Here we take inspiration from a toy, and describe an initial symmetry investigation of a new type of deployable structure that was invented by Hoberman [1], and is now sold as the ‘Hoberman Switch-Pitch’ (<http://hoberman.com/fold/Switchpitch/switchpitch.htm>). The Switch-Pitch changes between two different configurations, as shown in Figure 1(a-c). The ball-like configurations exist because of additional shell elements added to the outside of the basic structure, which is revealed when the shell elements are removed (Figure 1(d-f)). The basic structure consists of eight nodes, which are connected via links that have revolute joints at their ends. All the links at a node are synchronised by gears that ensure that they rotate together.

The mechanism of the Switch-Pitch has recently been investigated by Wei et al. [2], and Ding et al. [3]. They show that, for most configurations of the Switch-Pitch, the gearing is not necessary, but it is required to avoid singularities in the mechanism path when a node and its neighbours become coplanar. We follow the analysis of the simplified version as described in these papers, and neglect the role of the gearing.

One remarkable feature of the Switch-Pitch is its high symmetry, and in this paper we explore the use of a symmetry-adapted mobility rule [4] to understand the mobility of the structure. We also complete a simple first-order equilibrium/compatibility analysis, and use this with a predictor/corrector algorithm to show the deployment path of the structure.

2. Mobility analysis

2.1 Simple counting

From the formulation proposed by Hunt [5], and extended by Guest and Fowler [4], the relative mobility of an over-constrained structure can be obtained from the simple counting rule:

$$m - s = 6n - \sum_{i=1}^g (6 - f_i) - 6 \quad (1)$$

where m and s are the number of independent mechanisms and states of self-stress, n is the number of nodes, g is the number of bars, and f_i is the number of relative freedoms permitted by link i .

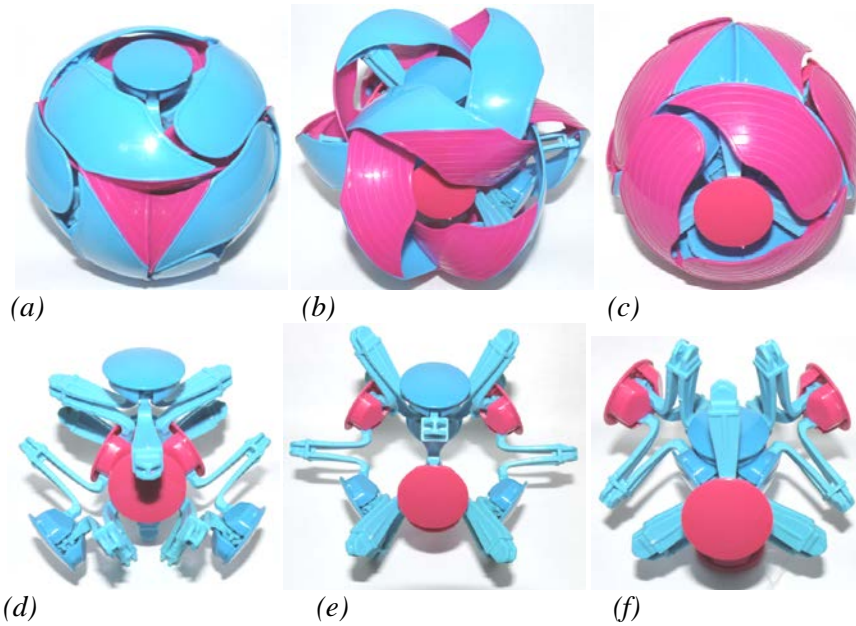


Fig. 1: The transformation of a Hoberman Switch-Pitch ball between two extreme configurations, (a) and (c). The internal structure is shown in (d), (e) and (f).

Figure 1 shows a physical model of the Hoberman Switch-Pitch, which consists of eight dome-shaped vertices, twelve \perp -shaped links, and twelve two-colored laminas. Each vertex has three intersecting revolute joints, and moves in and out during the transformation of the structure. By ignoring the laminas, and substituting the vertices and links as nodes and straight bars respectively, the ball structure can be transformed into the twelve-bar foldable structure shown in Figure 2-a. The structure consists of eight nodes ($n = 8$) and twelve elements ($g = 12$). Each element shown in Figure 2-b has a local coordinate system where the x -axis runs along the link, and the z -axis is orthogonal to a radial line from the centre of the structure. Each link allows two freedoms – the rotations about the local z -axis at each end connection, and hence $f_i = 2$ for all i . Therefore, the counting rule for this structure gives

$$m - s = 6 \times 8 - 6 \times 12 + 2 \times 12 - 6 = -6 \quad (2)$$

Thus, this equation does not reveal any information about possible motion of the structures, simply telling us of the existence of at least six states of self-stress.

2.2 Symmetry-adapted analysis

In fact, the Hoberman Switch-Pitch ball is highly symmetric, and more information about possible mechanisms can be obtained by counting symmetries, as well as components, of the polyhedral structure shown in Figure 2-a. Guest and Fowler [4] gave a symmetry-adapted

version of the counting rule given in Eq. (1), which is expressed in the language of representations as

$$\begin{aligned}\Gamma(m) - \Gamma(s) &= \Gamma(v) \times (\Gamma_T + \Gamma_R) - \Gamma_{\parallel}(e) \times (\Gamma_T + \Gamma_R) - (\Gamma_T + \Gamma_R) + \Gamma_f \\ &= [\Gamma(v) - \Gamma_{\parallel}(e) - \Gamma_0] \times (\Gamma_T + \Gamma_R) + \Gamma_f\end{aligned}\quad (3)$$

where $\Gamma(m)$ and $\Gamma(s)$ are the representations of the mobility, and the states of self-stress, respectively. $\Gamma(v)$ is the number of vertices unshifted by the symmetry operation, and $\Gamma_{\parallel}(e)$ is the representation of a set of vectors along the edges. Γ_T , Γ_R and Γ_f are the representations of total symmetry, rigid-body translations, rigid-body rotations, and joint freedoms, respectively, and Γ_0 is the totally symmetric representation.

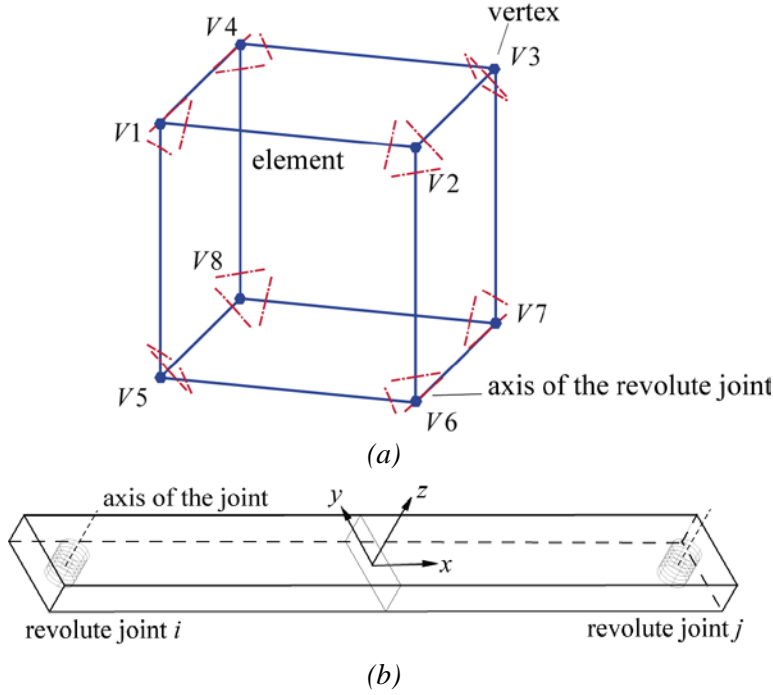


Fig. 2: (a) A representation of the underlying structure of the Hoberman Switch-Pitch as a cube. (b) a single element of the structure.

In its initial state, the structure shown in Figure 2-a has cubic symmetry (O_h), for which the character table is shown in Table 1. We evaluate equation (3) for the structure in tabular form, as used in Guest and Fowler [4]:

	E	$8C_3$	$6C_2$	$6C_4$	$3C_2$	i	$6S_4$	$8S_6$	$3\sigma_h$	$6\sigma_d$
$\Gamma(v, C)$	8	2	0	0	0	0	0	0	0	4
$-\Gamma_{\parallel}(e, C)$	-12	0	2	0	0	0	0	0	4	-2
$-\Gamma_0$	-1	-1	-1	-1	-1	-1	-1	-1	-1	-1
$=$	-5	1	1	-1	-1	-1	-1	-1	3	1
$\times (\Gamma_T + \Gamma_R)$	6	0	-2	2	-2	0	0	0	0	0
$=$	-30	0	-2	-2	2	0	0	0	0	0
$+\Gamma_f$	24	0	0	0	0	0	0	0	0	4
$= \Gamma(m) - \Gamma(s)$	-6	0	-2	-2	2	0	0	0	0	4

The novel row in this table is the evaluation of Γ_f , where we see that the character is zero under every operation except the identity (E), where all freedoms are preserved, and reflection in a plane that contains two bars (σ_d), where the four freedoms of the revolute

Table 1: The O_h character table, which gives the character of irreducible representations for each of the symmetry operations of the group.

O_h	E	$8C_3$	$6C_2$	$6C_4$	$3C_2$	i	$6S_4$	$8S_6$	$3\sigma_h$	$6\sigma_d$	Rotations, displacements
A_{1g}	1	1	1	1	1	1	1	1	1	1	
A_{2g}	1	1	-1	-1	1	1	-1	1	1	-1	
E_g	2	-1	0	0	2	2	0	-1	2	0	
T_{1g}	3	0	-1	1	-1	3	1	0	-1	-1	(R_x, R_y, R_z)
T_{2g}	3	0	1	-1	-1	3	-1	0	-1	1	
A_{1u}	1	1	1	1	1	-1	-1	-1	-1	-1	
A_{2u}	1	1	-1	-1	1	-1	1	-1	-1	1	
E_u	2	-1	0	0	2	-2	0	1	-2	0	
T_{1u}	3	0	-1	1	-1	-3	-1	0	1	1	(x, y, z)
T_{2u}	3	0	1	-1	-1	-3	1	0	1	-1	

Table 2: The T_d character table

T_d	E	$8C_3$	$3C_2$	$6S_4$	$6\sigma_d$	Rotations, displacements
A_1	1	1	1	1	1	
A_2	1	1	1	-1	-1	
E	2	-1	2	0	0	
T_1	3	0	-1	1	-1	(R_x, R_y, R_z)
T_2	3	0	-1	-1	1	(x, y, z)

hinges on the bars are preserved. Every other operation moves all of the revolute joints, hence leading to a zero character.

From the final row of the tabular calculation, $\Gamma(m) - \Gamma(s)$ can be written in terms of irreducible representations as

$$\Gamma(m) - \Gamma(s) = A_{2u} - A_{1u} - T_{1g} - T_{1u} \quad (4)$$

As both $\Gamma(m)$ and $\Gamma(s)$ must contain positive numbers of irreducible representations, this implies that

$$\Gamma(m) \supset A_{2u}, \text{ and } \Gamma(s) \supset A_{1u} + T_{1g} + T_{1u} \quad (5)$$

Thus, symmetry-adapted counting reveals the existence of a single mechanism, of symmetry A_{2u} . Displacing the structure along this A_{2u} path will reduce the symmetry from the cubic symmetry O_h , shown in Figure 3-a, to the tetrahedral symmetry T_d , shown in Figure 3-b.

To follow this path in the lower symmetry group, we repeat the evaluation of equation (3) in group T_d , for which the character table is given in Table 2. In fact, we can do this by re-using the former tabular calculation but using only the columns $E, 8C_3, 3C_2, 6S_4$, and $6\sigma_d$. In the group of T_d , $\Gamma(m) - \Gamma(s)$ can now be written as

$$\Gamma(m) - \Gamma(s) = A_1 - A_2 - 2T_1 \quad (6)$$

This evaluation reveals that at least one mechanism exists, and that $\Gamma(m) \supset A_1$.

Using a first-order geometric analysis, we will show later in Section 3 that only one mechanism exists. Therefore, we can conclude that

$$\Gamma(m) = A_1, \text{ and } \Gamma(s) = A_2 + 2T_1 \quad (7)$$

Thus, the mechanism along the path of full symmetry (A_1) must be a finite mechanism, as no equisymmetric state of self-stress exists [6].

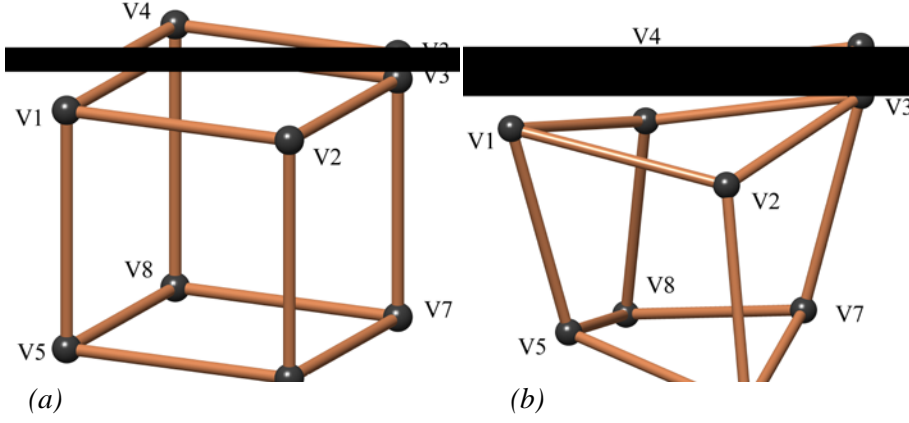


Fig. 3: The foldable structure: initial configuration (a) and a deformed configuration (b).

3. First-order analysis

To confirm that there is only one deformation path, an equilibrium matrix is generated. This matrix relates the equilibrium between external forces and moments applied at the nodes, and internal forces and moments in the structural elements. Consider an element k , as shown in Figure 2-b, which is connected by two revolute joints (i and j). It can carry axial forces f_{xk} , shear forces f_{zk} along direction z , torsion moments M_{xk} along direction x , and bending moments M_{yk} along direction y as shown in Figure 4; other loads cannot be carried because of the revolute joints connecting the element to the nodes.

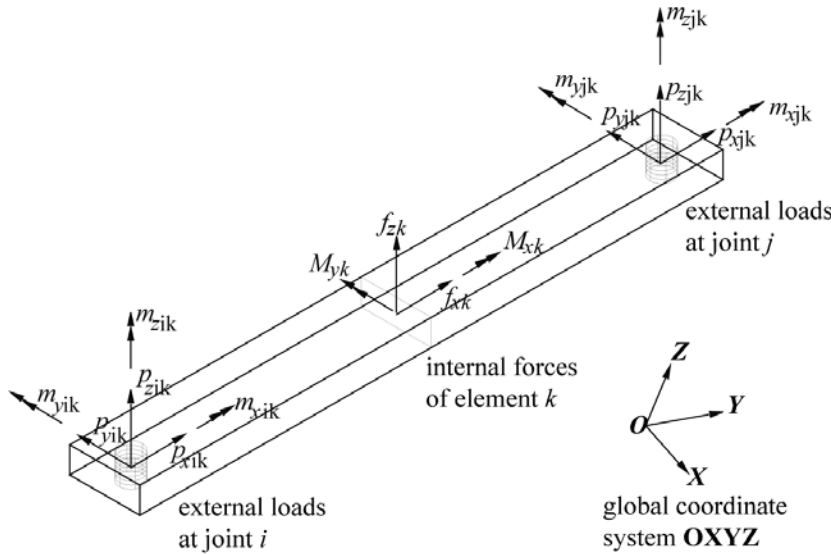


Fig. 4: An element k connected by revolute joints i, j

Thus we write

$$f_k = [f_{xk}, f_{yk}, M_{xk}, M_{yk}]^T \quad (8)$$

Now consider the external loads acting at node i or j that are in equilibrium with f_k . Define these loads in the local coordinate system (Figure 4) as being

$$P_{Ik} = [p_{xIk}, p_{yIk}, p_{zIk}, m_{xIk}, m_{yIk}, m_{zIk}]^T \quad I = i, j \quad (9)$$

Then the equilibrium of the element k in its local coordinate system can be expressed in a matrix form as:

$$\begin{bmatrix} h_{ki} \\ h_{kj} \end{bmatrix} f_k = \begin{bmatrix} P_{ik} \\ P_{jk} \end{bmatrix} \quad (10)$$

where

$$h_{kl} = \epsilon_I \begin{bmatrix} 1 & 0 & 0 & 0 \\ 0 & 0 & 0 & 0 \\ 0 & 1 & 0 & 0 \\ 0 & 0 & 1 & 0 \\ 0 & 0 & 0 & 1 \\ 0 & 0 & 0 & 0 \end{bmatrix} + L/2 \begin{bmatrix} 0 & 0 & 0 & 0 \\ 0 & 0 & 0 & 0 \\ 0 & 0 & 0 & 0 \\ 0 & 0 & 0 & 0 \\ 0 & 1 & 0 & 0 \\ 0 & 0 & 0 & 0 \end{bmatrix} \quad I = i, j \quad (11)$$

and ϵ_I is defined as -1 for joint i , and is $+1$ for joint j ; and L is the distance between the joints i and j .

There is a different local coordinate system for each element. Before considering the overall equilibrium matrix, we need to transform our equilibrium equation, so that all external forces and moments are stated in terms of the global coordinate system XYZ of the structure, which is also a right-handed system and shown in Figure 4. Transformation of axes from a local coordinate system to the global one can be summarized in matrix form as:

$$\begin{bmatrix} X \\ Y \\ Z \end{bmatrix} = R_0 \begin{bmatrix} x \\ y \\ z \end{bmatrix} = \begin{bmatrix} \cos(X, x) & \cos(X, y) & \cos(X, z) \\ \cos(Y, x) & \cos(Y, y) & \cos(Y, z) \\ \cos(Z, x) & \cos(Z, y) & \cos(Z, z) \end{bmatrix} \cdot \begin{bmatrix} x \\ y \\ z \end{bmatrix} \quad (12)$$

where R_0 is the 3×3 direction cosine matrix. For example, $\cos(X, y)$ from the matrix R_0 is the direction cosine of axis X with respect to local axis y . As there is no interference between forces and moments on transformation, the required transformation matrix R for the external loads and moments is:

$$R = \begin{bmatrix} R_0 & 0 \\ 0 & R_0 \end{bmatrix} \quad (13)$$

Hence,

$$H_{kl} = R \cdot h_{kl} \quad I = i, j \quad (14)$$

where H_{kl} is the equilibrium matrix of element k expressed in the global coordinate system.

For a complete polyhedral structure with n nodes and b elements, the full equilibrium matrix H can be generated from the global equilibrium matrices of all elements by conventional assembly techniques. The equilibrium equation for a polyhedral structure is:

$$H_{6n \times 4b} \cdot f_{4b \times 1} = P_{6n \times 1} \quad (15)$$

where the vector f contains the internal forces in every element, and the vector P contains the external forces at every node. We can use standard linear algebra techniques [7] to find states of self-stress and mechanisms for the structure.

The nullspace of H corresponds to solutions of $H \cdot f = 0$, i.e., states of self-stress, and has dimension

$$s = 4b - r \quad (16)$$

where s is the number of independent states of self-stress, r is the rank of the equilibrium matrix H . The compatibility equation could also be assembled in a similar way, and given as

$$C_{4b \times 6n} \cdot d_{6n \times 1} = e_{4b \times 1} \quad (17)$$

where the compatibility matrix, C , is the transpose ($C = H^T$) of the equilibrium matrix H , according to the principle of virtual work. The nullspace of C corresponds to solutions of $C \cdot d = 0$, and has dimension

$$m + 6 = 6n - r \quad (18)$$

where m is the number of internal infinitesimal mechanisms, to which we have added the six rigid-body modes that must exist as the structure is unconstrained.

In this work, the specific structure derived from the Hoberman Switch-Pitch ball has eight nodes and twelve elements, and the rank of the equilibrium matrix turns out to be $r = 41$. Therefore,

$$m = 6 \times 8 - 41 - 6 = 1, \text{ and } s = 4 \times 12 - 41 = 7 \quad (19)$$

which is in accord with the symmetry results.

4. Trajectory for the Switch-Pitch

We used the results from the first order analysis to follow the complete folding path for the Switch-Pitch structure, confirming the result that the structure should have a finite mechanism. To follow the path, a predictor-corrector algorithm was used, for which a schematic is show in Figure 5.

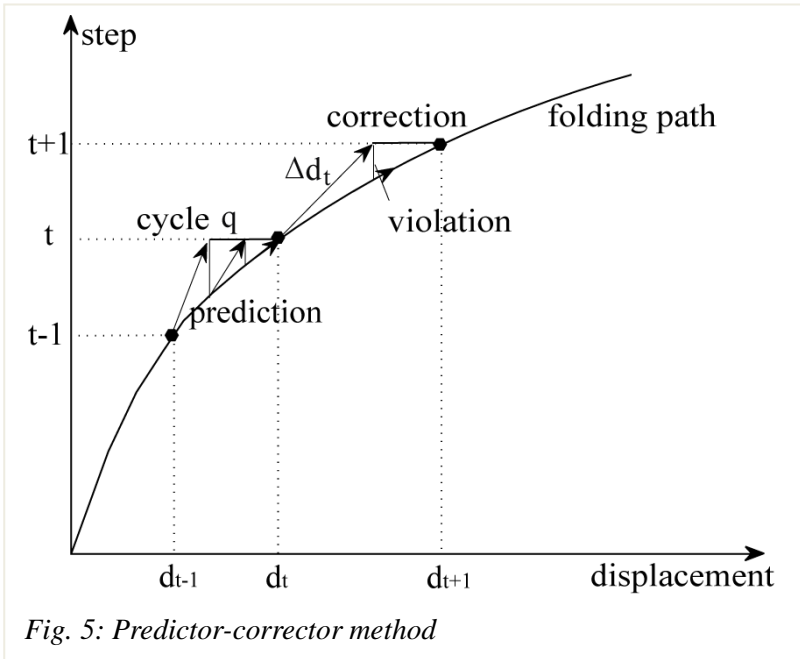


Fig. 5: Predictor-corrector method

At each step, the structure is displaced along the tangent to the folding path that is given by the non-rigid-body displacement in the nullspace of the compatibility matrix. As the path is non-linear, in the displaced configuration the length l_k of any member k is not identical to the original length l_{k0} , defining a strain that must be corrected. For example, the incompatible axial displacement e_k of member k is

$$e_k = l_k - l_{k0} \neq 0 \quad (20)$$

In fact, these are the only non-zero strains that need to be corrected, as none of the

nodes of the structure rotate along the folding path. Therefore, we can define the incompatible displacement matrix e of the structure as

$$e = [e_1, 0,0,0, \dots, e_k, 0,0,0, \dots, e_{12}, 0,0,0]^T \quad (21)$$

and a solution for the displacement required to correct the non-zero strain can be computed from Eq. (17) as

$$\delta d = -C^+ e \quad (22)$$

where C^+ is the generalized inverse matrix of the compatibility matrix.

The complete folding path of the Switch-Pitch mechanism is shown in Figure 6. Note that here we allow members to pass through one another; in practice, clashing would prevent the complete cycle being followed. In fact, as noted by Wei et al. [2], there are singular configurations where a vertex becomes co-planar with its neighbouring vertices, but we do not look carefully at those configurations here, and simply continue along the symmetric path.

5. Conclusion

We have shown that an understanding of symmetry has provided useful insight into the behaviour of the Switch-Pitch. However, more importantly, it has also suggested to us that

similar mechanisms based on other polyhedra will also be mobile, and we are currently working to develop more general mechanisms of this type.

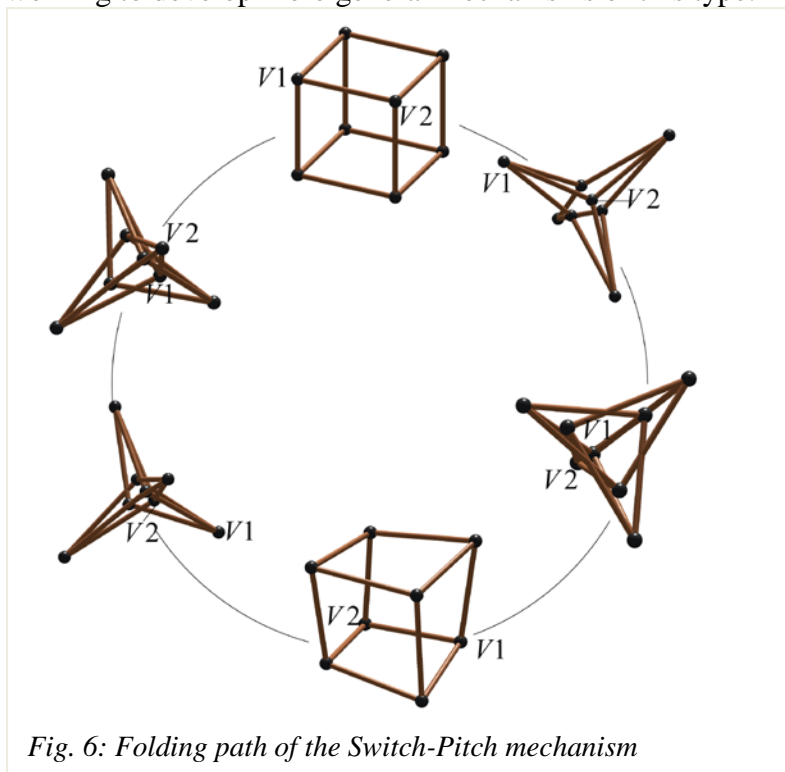


Fig. 6: Folding path of the Switch-Pitch mechanism

Acknowledgements

This study was carried out when the first author was visiting the Department of Engineering at the University of Cambridge. He is grateful for financial support from the China Scholarship Council and Scientific Research Foundation of Graduate School of Southeast University (Grant No. YBJJ1025) for this academic visit. We acknowledge partial funding support from a grant (code#06 R&D B03) from the Cutting-edge Urban Development Program funded by the Ministry of Land, Transport and Maritime Affairs of the Korean government.

References

- [1] HOBBERMAN C., "Geared Expanding Structures", U.S. Patent, App. No.: 10/743, 273, 2003.
- [2] WEI G.W., DING X.L., and DAI J.S., "Mobility and Geometric Analysis of the Hoberman Switch-Pitch Ball and Its Variant", *Journal of Mechanisms and Robotics (Transactions of the ASME)*, Vol. 2, No. 3, Aug. 2010, 031010 (9 pp).
- [3] DING X., YANG Y., and DAI J.S., "Topology and Kinematic Analysis of Color-changing Ball", *Mechanism and Machine Theory*, Vol. 46, No.1, 2011, pp.67-81.
- [4] GUEST S.D., and FOWLER P.W., "A Symmetry-extended Mobility Rule", *Mechanism and Machine Theory*, Vol. 40, No. 9, 2005, pp. 1002-1014.
- [5] HUNT K.H., *Kinematic Geometry of Mechanisms*, Clarendon Press, Oxford, 1978.
- [6] KANGWAI R.D., and GUEST S.D., "Detection of Finite Mechanisms in Symmetric Structures", *International Journal of Solids and Structures*, No. 36, 1999, pp. 5507-5527.
- [7] PELLEGRINO S., and CALLADINE C.R., "Matrix Analysis of Statically and Kinematically Indeterminate Frameworks", *International Journal of Solids and Structures*, No. 22, 1986, pp. 409-428.